Research Journal of Chemical Sciences _____ ISSN 2231-606X
Vol. **3(12),** 29-37, December **(2013)** *Res. J. Chem. Sci.*

Investigations of Nickel (II) removal from Aqueous Effluents using Electric arc Furnace Slag

Mohammed Yusuf*, Luqman Chuah A., Mohammed M.A. and Shitu A.
Department of Chemical and Environmental Engineering, Faculty of Engineering, University Putra Malaysia, 43400 UPM Serdang, Selangor DE, MALAYSIA

Available online at: www.isca.in, www.isca.me
Received 18th November 2013, revised 23th November 2013, accepted 13th December 2013

Abstract

The tendency of electric arc furnace (EAF) slag to the adsorb nickel(II) from aqueous solution has been investigated through batch experiments. Scanning electron microscopy (SEM), Fourier Transform Infrared Spectroscopy (FTIR) and Energy Dispersive X-Ray (EDX) Analysis. Analysis was characterized in order to give inside to the properties of electric arc furnace slag (EAFS). The adsorption result revealed that the maximum up take by the EAFS was 160.92mg/g at an equilibrium time of 216hr. The pseudo-second order kinetic fitted well with the kinetic data, showing a high determination coefficient (R^2) of over 0.996. The adsorption isotherms of nickel(II) on this adsorbent for both linear and non linear isotherms were well described by Langmuir model, this is because it shown a good fitting to the experimental data when compared to other isotherm models. Moreover the nickel(II) adsorption was found to be dependent on the adsorbent dosage, contact time and initial metal ion concentration. From the result it can be deduced that EAFS could be used to effectively adsorb nickel(II) from aqueous solution.

Keywords: Electric arc furnace slag, adsorption isotherm, sorption kinetics, nickel.

Introduction

The elimination of toxic heavy metals from aqueous environments has received considerable attention in recent years because of their toxicity and carcinogenicity[1]. Heavy metals such as lead, copper, manganese, cadmium, zinc, and nickel are among the common pollutants found in industrial effluents. They are usually non-degradable and tend to accumulate in the human body, causing various disorders[2]. Thus, heavy metals can cause severe physiological or neurological damage, even in small doses[3].

Copper is an essential nutrient, needed by the body in very small amounts. Short-term copper exposure can cause gastro-intentional disturbances, including vomiting and nausea. Copper mining, smelting, or municipal incineration can produce contamination of water with copper at concentrations above the permissible levels. The consumption of such water over a long period of time (years) causes liver or kidney damage[3].

Lead is a major pollutant as it has been commonly used as a raw material in battery manufacturing, printing, pigments, fuels, photographic materials, and explosives manufacturing[4]. The presence of lead in drinking water, even at low concentrations, may cause diseases such as anemia, encephalopathy, hepatitis, and nephritic syndrome [5].

Manganese is mainly used in steel-manufacturing industries with the aim of improving stiffness, hardness, and strength. It is also used in various types of products such as fireworks, dry-cell batteries, fertilizers, and paints. Exposure to high levels of manganese affects the respiratory tract and seriously disrupts brain function and control of the nervous system[6].

Nickel salts are commonly used in silver refineries, electroplating, zinc-base casting, storage-battery industries, printing, and production of alloys. These industries discharge significant amounts of a variety of nickel species into the environment[7]. According to the US Environmental Protection Agency (USEPA) requires nickel in drinking water should not exceed 0.04 ppm[8]. Therefore, it is necessary to reduce the concentration of heavy metals in industrial effluents to their permissible limit before these streams are discharged into the environment[9]. High concentrations of Ni^{2+} cause lung, nose, and bone cancers, headaches, dizziness, nausea and vomiting, chest pain and tightness, cyanosis, and extreme weakness[9]. Some nickel compounds such as nickel carbonyl are carcinogenic and easily absorbed by the skin. Exposure to this compound at an atmospheric concentration of 30ppm for an hour is lethal[10.] Current methods for nickel(II) removal and recovery from industrial waste streams include precipitation, oxidation, reduction, ion-exchange, reverse osmosis, solvent extraction, dilution, electrolytic extraction, adsorption, flocculation, sedimentation, evaporation and chelation, and biosorption, among others[11,12] .

The use of low cost adsorption technologies has been examined as a replacement for current expensive nickel removal methods[13]. Natural materials or waste products with a high adsorption capacity for heavy metals can be obtained from certain industries and subsequently employed and disposed of

with little cost. Electric arc furnace slag (EAFS) is a kind of slag obtained as a by-product in the steel-making industries. The majority of the end product is steel slag deposits, which generally cause environmental problems. Therefore, the development of methodologies for handling this slag is imperative. In addition, EAFS has been shown to serve as an adsorbent for the removal of manganese, copper, and chromium[6]. Herein, we have used EAFS as an adsorbent for nickel(II) because it is inexpensive and abundant, thereby making it ideal for low-cost treatment of wastewater. We studied the adsorption characteristics of nickel(II) on EAFS in a fixed-bed column by varying parameters such as inlet concentration, flow rate, and bed depth.

Material and Methods

Materials: The EAFS was obtained from a steel making plant (Southern Steel Berhad, (Panag, Malaysia). $NiCl_2{\cdot}6H_20$ was purchased from analytical Univar Reagents at APS Ajax. The solid reagents NaOH (99.95%), HCl (36.5%), and $KN0_3$ (99.98%) were supplied by Sigma Aldrich (St Louis, MO, USA).

Adsorbate preparation: A stock solution of nickel (1000 mg/L) was prepared by dissolving the desired quantity of $NiCl_2{\cdot}6H_20$ in distilled water. All the working solutions containing various concentrations were obtained by diluting the stock solution with distilled water. All the reagents used were of analytical grade.

Adsorbent preparation: The slag was first washed with distilled water in order to remove surface impurities, and subsequently dried at 100°C for 24h in an oven. The as-obtained EAFS was then crushed, ground, and sieved to obtain a uniform particle size of adsorbent (0.5 mm) for all the experiments in the present study.

Instrumentation: An atomic adsorption spectrophotometer (AAS, TAS 990 Shimadzu, Kyoto, Japan) was used for nickel(II) measurements. A peristaltic pump (PP 30, Miclins India, Limited, Chennai, India) afforded a constant flow of metal and desorbing solutions through the fixed column. A high precision electric balance (Sartorius GK3102, Germany) was used for weighing, and a digital pH meter (DHP-500, SICO, India) was used for pH measurements.

Results and Discussion

Characterization of adsorbent: Fourier Transform Infrared Spectroscopy (FTIR) Analysis: The FT-IR spectra of EAFS (Figure 1a and b) displayed a number of adsorption peaks, indicating complex nature of the material examined. An adsorption peak around 3920 cm^{-1} represented hydrated minerals such as $Ca(OH)_2$ and peak around 3771 cm^{-1} indicating the S-O stretch such as gypsum. The peak around 1559 cm^{-1} correspond to C-O a symmetric stretching, whereas a peak at 1472 cm^{-1} may be due to the bonding in CO_3^{2-} ion, which indicates the presence of some sort of carbonated mineral, possible due to the adsorption of CO_2 from the atmosphere. The peaks at 988 cm^{-1} and 874 cm^{-1} are Si-O and Al-O stretching while, peaks at 790 $cm^{-1}$to 709 cm^{-1} are due to C-O bonding 9 [9]. Shifting in peaks was observed after nickel(II) adsorption, this may indicate that these functional groups are likely to participate in the metal binding. A shift in hydroxide group from 3920 cm^{-1} to 3575 cm^{-1}, sulphonyl group from 3771 cm^{-1} to 3637 cm^{-1}, alcohol group from 1559 cm^{-1} to 1557 cm^{-1} while a shift in carbonate group from 1472 cm^{-1} to 1498 cm^{-1} was observed. The Al-O and Si-O stretching was observed which tends to shift from 988 cm^{-1} to 874 cm^{-1} and 1220cm^{-1} to 969 cm^{-1}, respectively. Finally, the C-O bonding shift from (790 cm^{-1} and 709 cm^{-1}) to (854 cm^{-1} and 812 cm^{-1}). The shift of these functional groups could correspond to the complexion and coordination of these groups with metal ion [14, 9].

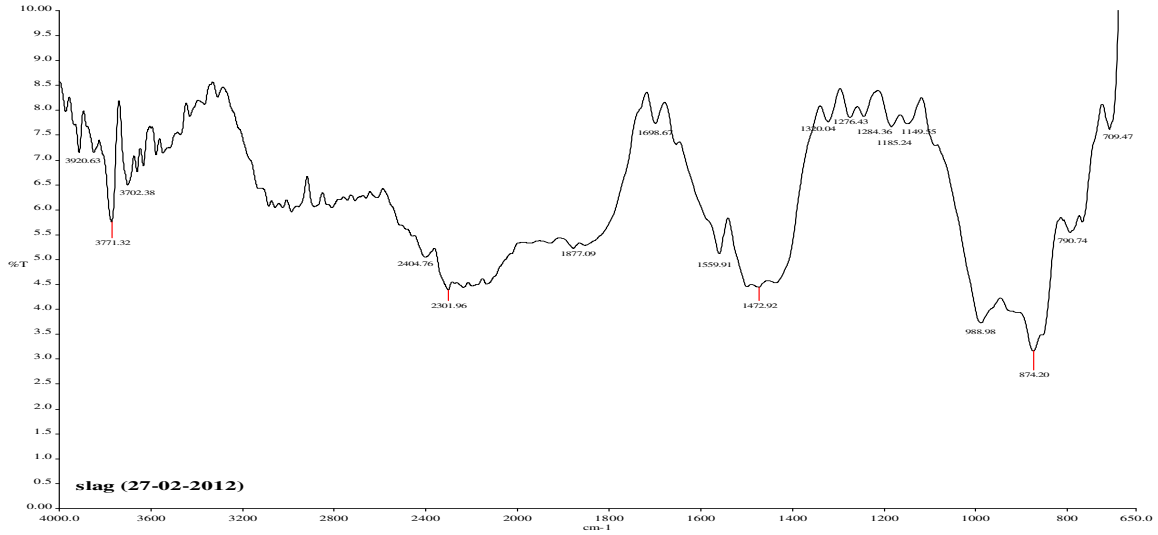

Figure-1a
FTIR spectra before adsorption has taken placed

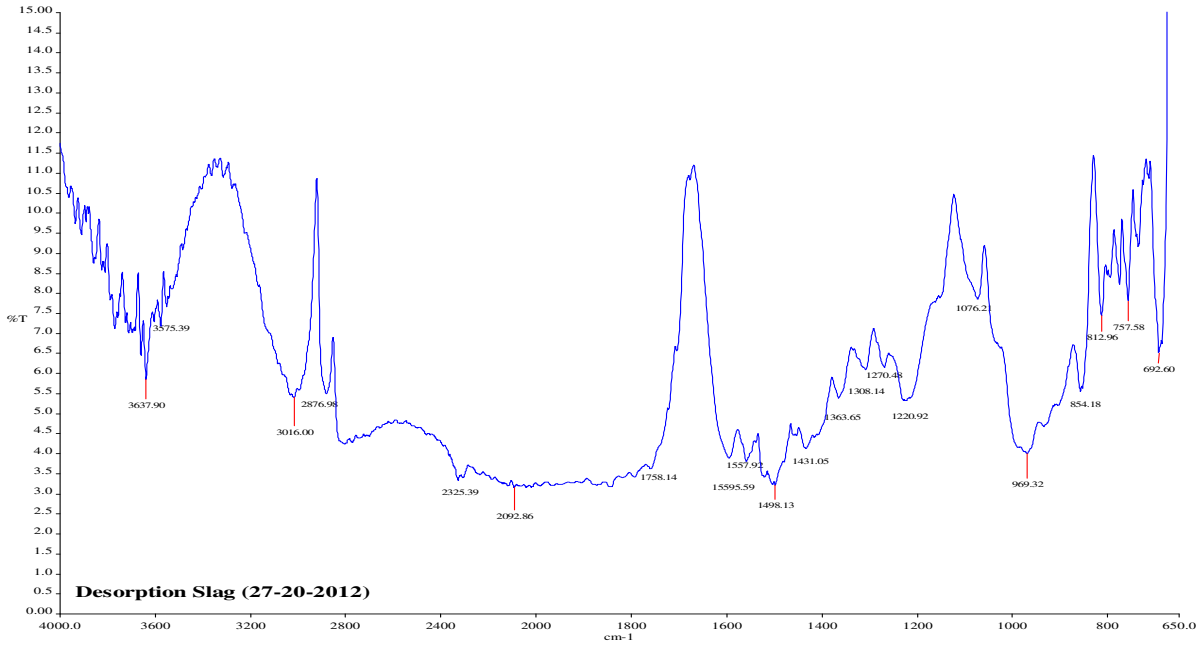

Figure-1b
FTIR spectra after adsorption has taken placed

Energy Dispersive X-Ray (EDX) Analysis: The energy dispersive X - ray spectrometer (EDX) is a quantitative analysis which is used to understand the chemical composition of EAF slag and the presence of Fe K which has the highest percentage by weight of 34.18 % and it decrease to 9.99 % after the adsorption has taken place, it can also be seen from table 4.2 that there is no any amount of Ni K present before the adsorption has taken place, but after the adsorption the percentage by weight becomes 27.94 %. Further more from the EDX analysis it shows that the element Mn K and O K decreases in their weight percentage from (4.29 to 1.67 %) and (14.67 to 4.29 %) for before and after adsorption respectively. Mg K and AL K also decrease in their percentage weight (1.39 to 0.99 %) and (6.11 to 2.0 %) for both before and after adsorption respectful. The only element that increases in the weight percentage are C K, Si K and Ca K to a value s of (6.27 to 9.73 %), (94.67 to 10.72 %) and (26.95 to 31.77 %) respectively.

Boehm's acid-base titration: Boehm's acid-base titration studies showed presence of 0.787 mmol/g acidic groups (carboxylic – 0.342 mmol/g, phenolic – 0.445 mmol/g) and 0.011 mmol/g basic groups. Results confirm dominance of acidic functionalities over EAFS surface.

Scanning Electron Microscopy (SEM) Analysis: The Scanning electron microscopy (SEM) was used to examine the morphology of the adsorbent (EAFS) samples before and after adsorption. It was found that the EAFS to be porous and irregular in structure with a bigger pore structure of 1.55-2.12 µm before adsorption which decrease to 0.17-0.40 µm after adsorption, thus favoring the adsorption of nickel(II) on different parts of the adsorbent. Figures. 2a and b show the SEM images of the EAFS before and after adsorption, respectively.

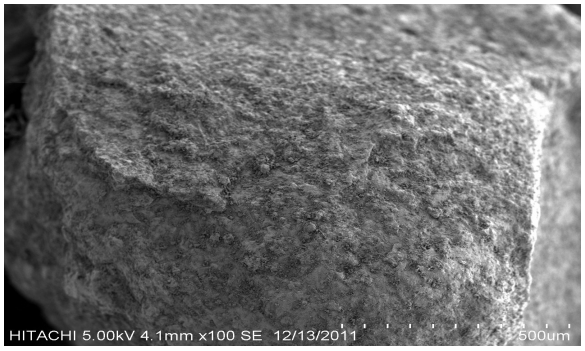

Figure-2a
SEM before adsorption has taken placed

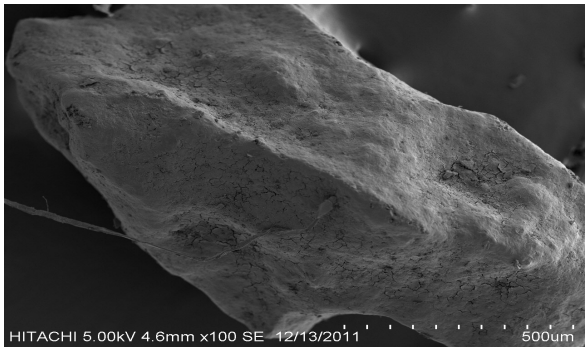

Figure 2b
SEM after adsorption has taken placed

Effect of dosage: Adsorbent dose have a great influence in the adsorption process. The effect of EAFS dose on nickel(II) adsorption was studied at a room temperature of 28^0C, optimum pH: 8 and initial nickel(II) concentration 100 mg/L. The increase in EAFS dosage from 0.1 to 1g resulted in an increase in adsorption of nickel(II) from 3.5 to 82.1%, respectively as shown in figure 3. An increase in adsorption might be due to the increase in adsorbent surface and therefore more active functional groups resulting in the availability of more binding sites for nickel(II) adsorption[15]

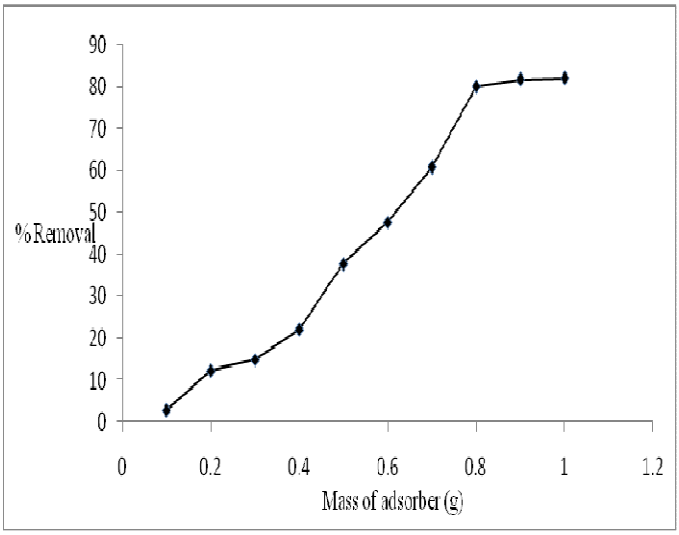

Figure-3
Effect of EAFS dose on Ni (II) adsorption

Effect of pH: The consequence of solution pH was considered as an important parameter in the adsorption process especially in aqueous solutions[9]. This is because hydrogen ion competing with positively charge metal ion on the active site of the adsorbent[16]. The effect of pH on adsorption of nickel(II) on EAF slag has been studied by varying the ranges from 2 to10 respectively, with an initial concentration of 100 mg/L, 1 g of EAFS, at room temperature and agitation speed of 150 rpm. Adsorption capacity of 77.49 % was achieved at a pH 8. The nickel intake was found to increase from pH 2 to 8 and start decrease as the pH goes higher. Furthermore between pH ranges of 6 to 8, there is a sharp increase in the amount of nickel removed, this may be due the formation of nickel hydroxide normally start in this ranges of pH. Below the pH, nickel (II) is in ionic form and for pH value greater than 8. It was observed that the pH of the solution will be slightly increased from 8 to 9; this may be due to the formation of CaOH from CaO present in the slag. Therefore the removal of nickel start to decrease from the pH of 9 to 10 this is as a result of chemical precipitation of the metal ion inform of hydroxide as shown in figure 4.

Effect of particle size: Particles with a different surface area have different adsorption capacity and size[17]. At fixed nickel(II) concentration - 100mg/L and varying EAFS particle size (0.5, 1, 2 and 3 mm), the effects of EAFS particle size on nickel(II) adsorption was investigated. The working condition of agitation speed of 150 rpm, contact time of 9 days and pH: 8 were kept constant. From the results it revealed that the percentage removal of nickel (II) tend to increase from 23 to 82% with decrease from 3to 0.5 mm, respectively figure 5. Larger particle size has a longer diffusion path, while smaller particle has a shorter diffusion path, thus allowing the adsorbate to penetrate quickly and deeply into the adsorbent particles resulting to higher rate of adsorption. Also, there is a possibility of intra-particle diffusion from the outermost surface into the pores of the material. As the particle size increases the diffusion resistance to mass transfer becomes greater, this is due to various factors, such as contact time, diffuse path and blockage in sections of the particles resulting in lowering in adsorption [17].

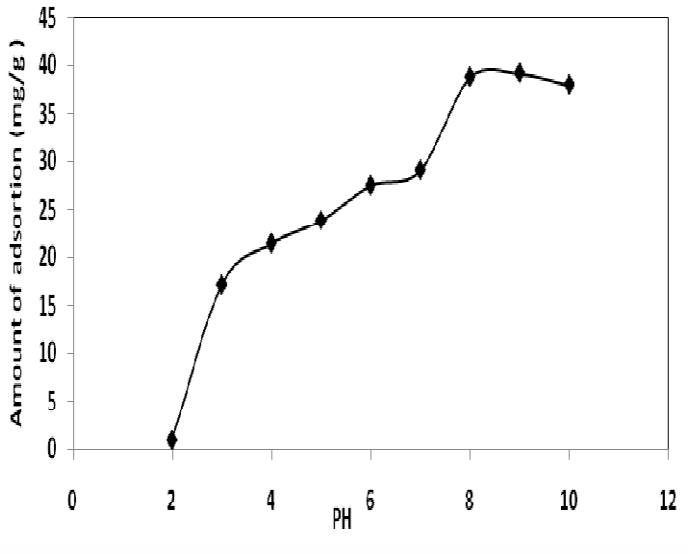

Figure-4
Effect of pH on nickel (II) removal on electric arc furnace slag

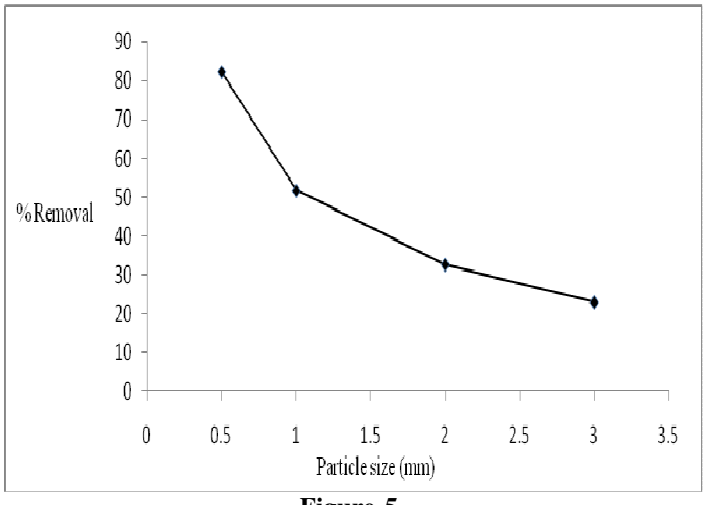

Figure-5
Effect of EAFS particle size on nickel(II) adsorption

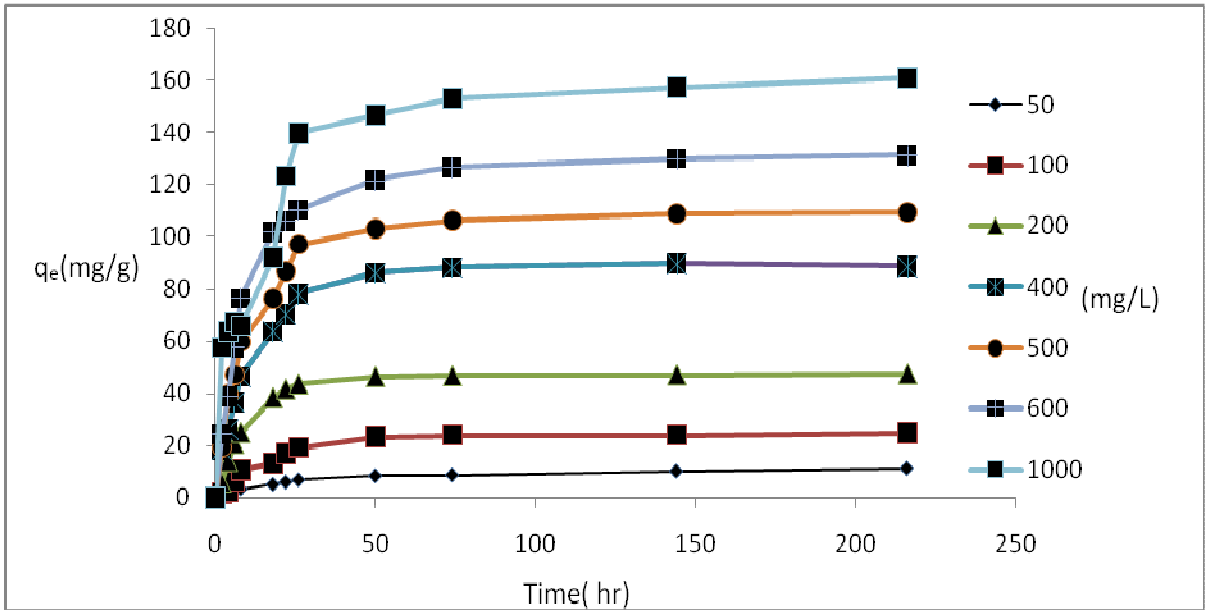

Figure-6
Effect of contact time and different initial concentrations on nickel adsorption

Effect of time and concentration: The hidden motive that plays an important role to overcome all the mass transfer resistance of nickel(II) between solid phase and aqueous phase is provided by the initial metal ion concentration. The initial metal ion varies from 50 to 1000 mg/L. As the initial nickel(II) concentration increases from 50 to 1000 mg/L, the amount of adsorption also increased from 11.2 to 160.9 mg/g, also with the increased in the percentage of nickel(II) adsorbed per unit mass of the adsorbent to increase in value from 73.8 to 83.0%. The highest adsorption of nickel(II) was said to occur at 26 h and thereafter increases slowly until it reached the equilibrium point of 216 h and that is the point at which adsorption tend to be constant. Higher rate of percentage removal was observed at the beginning, this is due to a large surface area of the slag being available for the sorption of the metals[18]. At a time interval of 0 to 26 hr a rapid adsorption was observed, this is because of the availability of the active sites on the absorbent surface which is usually decreases with time therefore, there is less change of adsorption[19]. Figure 6 shows the plots representing the amount of adsorbate adsorbed versus the contact time for the initial metal ion concentration.

Effect of Agitation speed: In order to determine optimal agitation speed experiments were conducted by varying agitation speed at pH: 8 and initial nickel(II) concentration - 100mg/L. As the agitation rate increases from 180 to 300 rpm the EAFS adsorption capacity increases from 20.52 to 24.49 mg/g, respectively. This indicates that nickel(II) diffusion from solution to the surface of adsorbent and into the pores increased with the increase in agitation rate[19].

Adsorption isotherm studies: The arithmetical models that illustrate the distribution of the adsorbate species among adsorbent and liquid is known as the adsorption isotherm [20]. Among the widely used linear models are the two parameter models, they include Langmuir, Freundlich and Temkin isotherm. These isotherms function by describing the equilibrium adsorbate concentration in the bulk fluid phase C_e, to the metal uptake per unit mass of adsorbent q_e.

Langmuir isotherm based it assumption that the optimum adsorption occur when saturated monolayer of solute molecule is present on the adsorbent surface [21]. There is no migration of adsorbate molecules in the plane surface and the energy of adsorption is constant. The Langmuir isotherm is express in [1] [22]

$$\frac{C_e}{q_e} = \frac{1}{k_L} + \frac{a_L C_e}{k_L} \qquad (1)$$

Where C_e is the equilibrium concentration of the adsorbate (mg/L), q_e is the amount of adsorbed under equilibrium (mg/g), $\frac{1}{k_L}$ is the point of interception, $\frac{a_L}{k_L}$ and is the slop of the plot. a_L and k_L are determined from the slop of and intercept of the plot.

For heterogeneous surfaces and multilayer sorption, the Freundlich isotherm models is often used, assuming different site with several adsorption energies are involved. The relationship that exists between the concentrations of the nickel at equilibrium C_e and the amount of nickel adsorbed per unit

mass of adsorbent q_e was shown by the Freundlich adsorption isotherm. A linear form of the Freundlich equation is given as [23].

$$Lnq_e = Lnk_F + \frac{1}{n} LnC_e \quad (2)$$

Where C_e is the equilibrium concentration of adsorbate mg/L, q_e is the amount of adsorbate adsorbed under equilibrium mgg^{-1}, k_f and n are the Freundlich constant (mg/L), $\frac{1}{n}$ is the heterogeneity factors. The parameters are presented in Table 1.

Table-1
Linear parameters of two models Langmuir and Freundlich

Langmuir		Freundlich	
Al	0.0091	1/n	0.6304
Kl	1.8570	kf	4.4781
R^2	0.9961	R^2	0.9519

The Langmuir type of isotherm shows the surface homogeneity of the adsorbent while the Freundlich type adsorption isotherm shows an indication of surface heterogeneity of the adsorbent. Furthermore the Freundlich isotherm gives no information on the monolayer adsorption capacity in contrast to the Langmuir model. From the corresponding values of R^2, when compared it shows that Langmuir isotherm is the best model for nickel since it fitted well with the correlation coefficient of 0.9961 higher than that of the Freundlich which is 0.9519, this is demonstrated in figure 7. The isotherm equations were applied to find the best curve fitting using non-linear correlation coefficient and the four error function. By comparing the experimental adsorption data with the non-linear plot of Langmuir, Freundlich and Redlich-Peterson model as shown in figure-7.

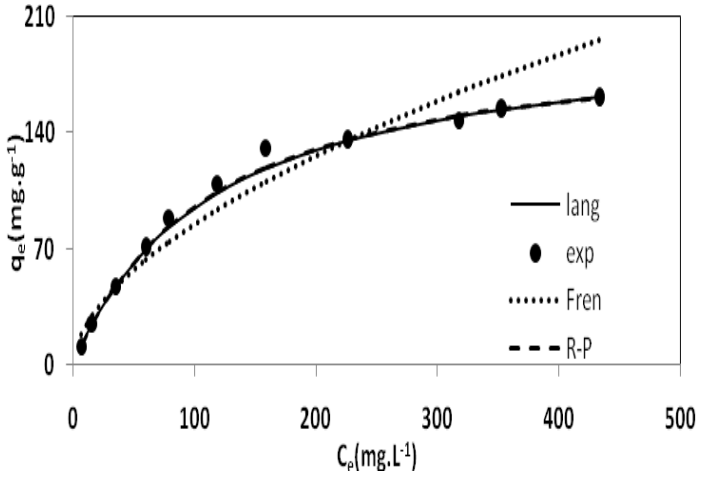

Figure-7
A comparison between experimental data with non-linear models of Langmuir, Freundlich and Redlich-Peterson

Langmuir model shows the most suitable model followed by Redlich-Peterson and the least was the Freundlich model. On the basis of R^2 values and the error functions values for the non-linear model the best was found to Langmuir>Redlich-Peterson> Freundlich model. The trial and error methods was used to minimized the error function using the Microsoft excel software (solver), by minimizing the error function across the ranges provided by the experimental concentration of the isotherm parameter. On the basis of the lowest value of the error functions Standard Error Estimate (SEE) and Average Relative Error Function (ARE) and the highest correlation coefficient data R^2, the highest correlation coefficient value R^2 of 0.9999 was obtained from both Langmuir and Redlich Peterson model, while Freundlich model show the lowest correlation coefficient value R^2 of 0.9456. For SEE error function, the lowest error value of 4.56 was obtained from Langmuir model, while Redlich- Peterson and Freundlich model each has the error value of 14.27 and 23.17 respectively. Moreover in the case of ARE error function, the lowest error value of 3.83 was obtained from Redlich-Peterson model followed by Langmuir model which has the error value of 4.05 while Freundlich has the highest error value of 14.12. From the result obtained it can be deduced that Langmuir model shown the lowest error value when compare with the Redlich-Peterson and Freundlich model. The table 2 shows the isotherm parameters and their error functions.

Table-2
Non-linear parameters of isotherm models with their error functions

Isotherm model	Parameters			Error function	
			R^2	SEE	ARE
Langmuir	K_L	0.008568	0.9999	4.56	4.05
	q_m	205.3952			
Freundlich	K_F	6.153656	0.9456	23.17	14.12
	1/n	0.570308			
Redlich–Peterson	K_{PR}	0.008069	0.9999	14.27	3.83
	q_{PR}	216.7668			
	B	1.008946			

Kinetic study: The pseudo-first-order rate model equation was originally formulated by Lagergren[24]

$$\frac{dq_t}{dt} = k_1 \ (q_e - q_t) \quad (3)$$

Where q_e is the amount of solute adsorbed at equilibrium per weight of adsorbent (mg/g), q_t is the amount adsorbed at any time (mg/g) and k_1 is the adsorption constant and then equation (5) is arranged to give to give a linear time dependence functions as

$$Log(q_e - q_t) = Log(q_e) - \frac{K_1 t}{2.303} \quad (4)$$

Where q_e is the amount adsorbed at equilibrium, q_t is the amount adsorbed at equilibrium (mgg^{-1}) at time t, k_1 is the rate constant of the pseudo-first-order adsorption process (min). To obtained the constant value k_1 a straight line plots of $log\ (q_e - q_t)$ against t were used. The correlation coefficients R^2 for different nickel(II) concentration as shown in figure 8 has the coefficient of 0.951 (for 50mg/L) to 0.928 (for 1000mg./L), and from the calculated value of adsorption capacity (q_{cal}) the following values were obtained 11.2mg/g for (50mg/L) to 160.92mg/g for (1000mg/L). It was observed that nickel(II) on electric arc furnace slag did not follow the pseudo-first-order kinetic when compare with the pseudo-second order kinetic.

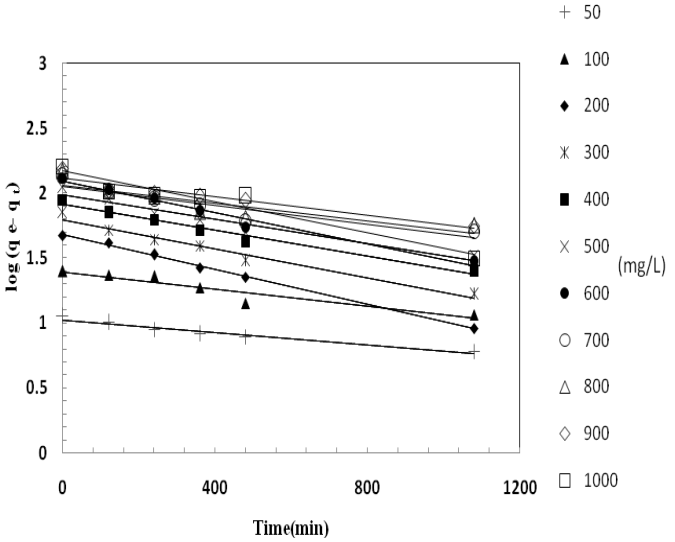

Figure-8
Pseudo-first-order models in different initial concentrations on nickel adsorption

In the Pseudo-second-order model, Lagergren equation was also used to determine the rate constant for the adsorption of nickel(II) on slag. The differential equation for this reaction as modified by Ho and McKay [25] is given below

$$\frac{dq_t}{dt} = k_2(q_e - q_t)^2 \quad (5)$$

By integrating the above equation at a boundary condition t=0 to › 0 and q=0 to › 0 and rearranging to obtain the liberalized form as shown in equation (7) as given:
By substituting $k_2q_e^2$ with h the pseudo-second-order equation can be expressed as:

$$\frac{t}{q_t} = \frac{1}{h} + (\frac{1}{q_e})t \quad (6)$$

Where q_t is the amount adsorbed ($mg.g^{-1}$), q_e is the amount adsorbed at equilibrium ($mg.g^{-1}$), t is the time in (min), k_2 is the rate constant of pseudo-second-order adsorption ($g.mg^{-1}min^{-1}$). The plot of $\frac{t}{q_t}$ versus t should give a straight line if pseudo-second-order kinetic is to be useful. From the plotted graph k_2 and h are obtained from the slop and intercept of the plot respectively. The linear form of pseudo-second-order kinetic at different nickel(II) concentration on slag is shown in figure 9.The correlation coefficient R^2 for the pseudo-second-order kinetic at different concentration was 0.996 (for 50mg/L) to 0.974 (for 1000mg/L) while the calculated values of adsorption capacity (q_{cal}) tend to be higher than that of the pseudo-first-order kinetic, its value ranges from 11.9 (for 50mg/L) to 161.3 (for 1000mg/L) at different concentrations.

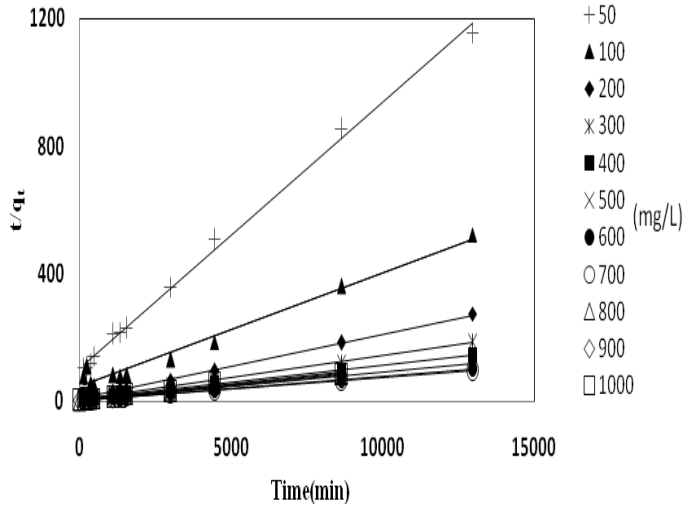

Figure-9
Pseudo-second-order models in different initial concentrations on nickel adsorption

The plots showed a high correlation coefficient (R^2) which shows a good compliance with the pseudo-second-order equation. The data obtained also show that increase in the initial concentration resulted to the increase in initial sorption rate values. The lower the concentration of the nickel ions in the solution, the lower the collision rate between the species the faster the nickel ion bounded to the active sites on the surface of the adsorbent. However do to large number of nickel ion adsorbed at the available adsorption sites, resulted to increased in the initial nickel ion concentration and also increased in the equilibrium adsorption capacity q_e. Comparing the correlation coefficient (R^2) for both pseudo-first-order and pseudo-second-order equation, it can be observed that the correlation coefficient (R^2) for the pseudo-first-order equation are lower than that of the pseudo-second-order equation coefficient, this gives a strong indication that the sorption of nickel(II) by the electric arc furnace slag more accurately presented by the pseudo-second-order kinetic process. In addition, the comparison of the second-order kinetic model with the inter-particle diffusion model shows that the intra-particle diffusion model is less suitable for representing the experimental data, as shown in figure 10. This is because the diffusion of the metal species into pores is a prevailing factor controlling the mechanism of the adsorption[23].

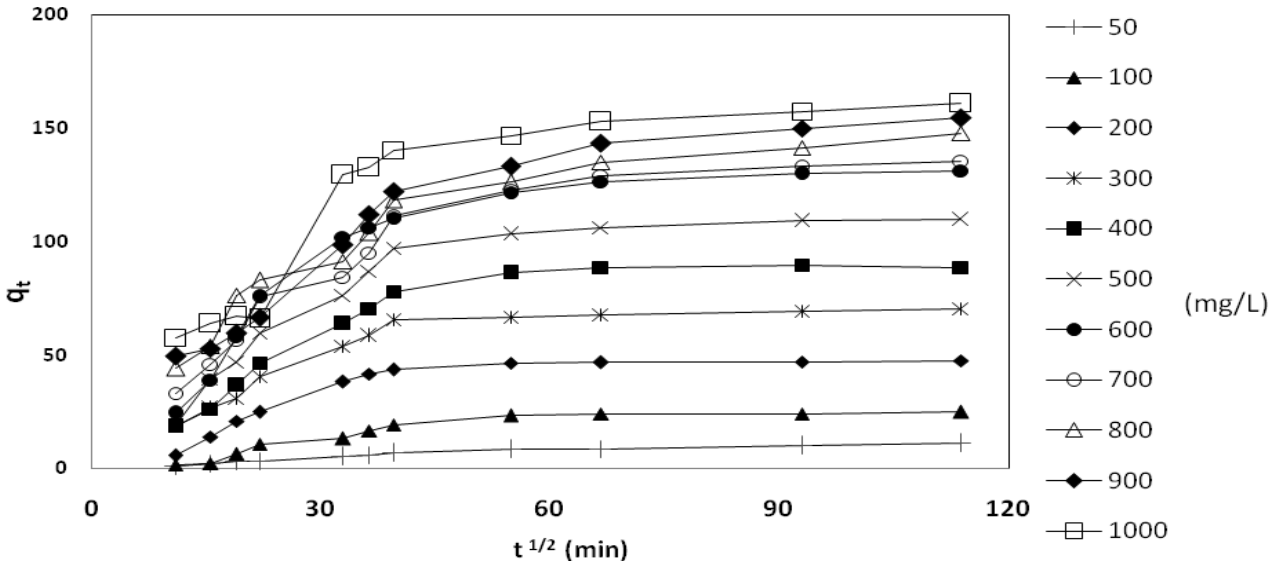

Figure-10
Intra-particle diffusion model at different initial concentration on nickel adsorption

Conclusion

The results showed that the potential use of electric arc furnace slag for the adsorption of nickel(II) from aqueous solution. The amount of nickel(II) adsorbed into the EAF slag increases with an increased in concentration and dosage of adsorbent, in addition the adsorption of nickel is dependent on the initial metal ion concentrations of the adsorbent, adsorbent dosage, time of contact and pH. Maximum percent removal of nickel(II) is at pH 8, while the minimum is at pH 2. It was found that the kinetics of the adsorption of nickel(II) on EAF slag obeyed pseudo-second-order equation with a good correlation. The adsorption isotherm followed the Langmuir model due to the fact that it shown a good fitting to the experimental data when compare with other isotherm models. Finally It can be deduced that the EAF slag,a residue from steel plant which readily available and easy to obtained at low cost, is a suitable adsorbent for the removal of nickel ion from aqueous solution and waste water.

Reference

1. Littui H., Yuan Yuan, S., Tao Y., Li L., Adsorption behavior of Ni (II) on Lotus stalk derived active carbon by phosphoric acid activation, *Desalination*, **268,** 12-19 **(2011)**

2. Rifaqatu, A.K., Moonish A.K., Removal and recovering of Cu(II), Cd (II) and Pb (II) ions from single and multi metal system by batch and column operation on neem oil cake (NOC), *Separation and Purification Techn*ology, **57,** 397-402 **(2007)**

3. Mohan, S., Streelakshmi G., Fixed bed column study for heavy metal removal using phosphate treated rice husk, *J. of Hazard Mater.*, **153**, 253-262 **(2008)**

4. Jalali R., Ghafourian H., Asef, Y., Davarpanah, S. J., Sepehr S., Removal and recovery of lead using non living biomass of marine algae, *J. of Hazard Mater.*, **B 2,** 253-262 **(2002)**

5. Nlo H., Chua K.H. and S.H.B. Lam, A comparative investigation on the biosorption of lead by filamentous fungal biomass, *Chemosphere*, **39**, 272-2736 **(1999)**

6. Beh C., Chuah L., Choong T.S.Y.,. Kamarudzaman M.Z.B. and Abdan K., Adsorption study electric arc furnace slag for the removal of manganese from solution, *American Journal of Applied Sci.,* **7(4),** 442–446 **(2010)**

7. Chungsying L., Comparisons of sorbent cost for the removal of Ni^{2+} from aqueous solution by carbon nanotubes and granular activated carbon, *J. of Hazard Mater.*, **151**, 239-246 **(2008)**

8. Xue S.W. and Yong Q., Removal of Ni(II), Zinc(II) and Cr(VI) from aqueous solution by Alternanthra philoxeroides biomas, *J. of Hazard Mater.*, B138, 585-588 **(2006)**

9. Malkoc E., Ni (II) removal from aqueous solutions using cone biomass of Thuja orientalis, *J. of Hazard Mater.*, **137**, 899-908 (**2006)**

10. Vieira M., Neto A., Gimenes M, M. da Silva, Sorption kinetics and equilibrium for the removal of nickel ions from aqueous phase on calcined Bofe bentonite clay, *J. of Hazard Mater.*, **177**, 362–371 **(2010)**

11. Crini G., Recent developments in polysaccharide based materials used as adsorbents in wastewater, treatment. Proly. Sci., **30**, 38-70 **(2005)**

12. David W.O., A modified cellulose adsorbent for the removal of nickel (II) from aqueous solution, *Journal of*

Chemical Technology and Biotechnology., **81**, 1820-1828 **(2006)**

13. Dimitrova S.V., Use of granular slag column for lead removal, *Water Resource*, **36**, 4001–4008 (**2002)**

14. Yanli M., Hongwei H.Y. and Hongxian O., A novel extracellular biopolymer produced from pseudonas fluoresces C-2 preparation, characterization and adsorption behaviours toward nickel (II) ions in aqueous solution, *Inter. J. Mat Str Integration*., **6**, 74-93 **(2012)**

15. Kumar P.S.; Kirthika K. Equilibrium and kinetic study of adsorption of nickel from aqueous solution ontobael tree leaf powder, *J. Eng. Sci. and Tech.,* **40**, 351-363 (**2009)**

16. Bernard E., Jimoh A. and Odigure J.O., Heavy metal removal from industrial wastewater by activated carbon prepared from coconut shell, *Res. J. Chem. Sci.,* **3(8),** 3-9 **(2013)**

17. Malkoc E., Nuhuoglu Y., Removal of Ni(II) from aqueous solution using waste tea factory: Adsorption on a fixed-bed column, *J. of Hazard Mater.*, **40**, 326-336 **(2006)**

18. Alka T. and Prerma K., Superparamagnetic PVA-Alginate microspheres as adsorbent for Cu^{2+} ion removal from aqueous system, *Int. Res. J. of Environ Sci.,* **2(7)**, 44-53 **(2013)**

19. Ozacar M. and Sengil A., Adsorption of complex dyes from aqueous solution by pine sawdust, *J. Bioresource Technol.,* **7,** 791-795 **(2005)**

20. Lu C., Liu C. and G.P. Rao, Comparisons of sorbent cost for the removal of Ni^{2+} from aqueous solution by carbon nanotubes and granular activated carbon, *J. of Hazard Mater.*, **151**, 239-246 **(2008)**

21. Carvalho W.A., Vignado C. and Fontana J., Ni(II) removal from aqueous effluents by silylated clays, *J. of Hazard Mater.*, **153(3),** 1240–1247 **(2008)**

22. Ofomaja A. E., Intraparticle diffusion process for lead (II) biosorption onto mansonia wood sawdust, *J. Bioresource Technol.,*, **101(15),** 5868–5876, **(2010)**

23. Freundlich H., Uber Die, Adsorption in lunsungen, *Journal of Physical Chemistry,* **57**, 347– 470 **(1985)**

24. Lagergren S., About the theory of so-called adsorption of soluble substances, Kungliga Svenska Vetenskapsakademiens Handlingar, **24 (4),** 1–39 **(1898)**

25. HoY., Ng J., McKay G., Kinetics of pollutant sorption by biosorbents: review, *Separation Purification Technology*., **29(2),** 189–232 **(2000)**